A NEW TECHNIQUE FOR DISTINGUISHING INTERNAL VOIDS FROM SOLID INCLUSIONS

K. I. Maslov, T. Kundu* and O. I. Lobkis

Institute of Chemical Physics, Russian Academy of Science
Kosygin Str.4, 117334 Moscow, Russia

*Department of Civil Engineering and Engineering Mechanics
University of Arizona, Tucson, AZ 85721, USA

INTRODUCTION

An acoustic microscope has been proven to be a very effective tool for visualization and characterization of small internal defects in solids[1]. The distinction of internal defects such as cracks and voids from solid inclusions is sometimes necessary for material evaluation. For example in case of light metal casting alloys ultrasonic scattered echo from pores and heavy metal inclusions used for strengthening purposes can give the ultrasonic signal of the same order of magnitude [2]. In this paper it is shown how the phase information of the reflected echo can be used to distinguish void signals from solid inclusion signals. Conventional acoustic imaging techniques that use only amplitude information and ignores the phase information can not distinguish between voids and inclusions.

It is well known that the phase of the acoustic wave reflection coefficient of a boundary is determined by the ratio of the acoustic impedance of the two media adjacent to the boundary [3]. However in case of hidden defects in a material it is not easy to determine experimentally the exact value of the phase of reflection coefficient due to the unknown distance of the defect. The phase shift is also affected by the defect geometry and by the transmission of the wave at the liquid-solid interface.

Application of the time-frequency domain analysis [4] and phase spectral analysis [5] to characterize the object under inspection has been widely discussed in the literature. It has been theoretically shown that the absolute phase shift and the relative acoustic impedance of the obstacle can be determined using these techniques. Recently, combined acoustic microscopy and acoustic spectroscopy techniques have been used to determine the complex value of reflection coefficient of a bulk material with a flat surface [6].

In the present paper we develop a method to distinguish spherical voids from solid inclusions by the phase-frequency dependence analysis.

Review of Progress in Quantitative Nondestructive Evaluation, Vol. 15
Edited by D.O. Thompson and D.E. Chimenti, Plenum Press, New York, 1996

THEORY - ACOUSTIC MICROSCOPY OF SPHERICAL INCLUSIONS.

The solution of the scattering of plane acoustic waves by a spherical inclusion in a solid has been given by Ying and Truell [7] and Einspruch et. al. [8]. The simplified expressions [9] and the solution for ultrasonic pulse [10] are also available in the literature.

Attempts have been made to obtain the expression of the scattered signal from the spherical inclusion for a focused transducer [11,12]. The theory of acoustic microscopy of a spherical particle in an immersion liquid and spherical void in a solid have been presented by Lobkis et.al. [12,13]. This theory relevant to this paper is briefly reviewed here, omitting the details.

The output signal generated by the focused beam scanning of this object has been analytically obtained by Lobkis, Kundu and Zinin [14]. The analytical solution was obtained only after several simplifying assumptions were made. First, the duration of the RF signal of the microscope is long enough to justify the continuous wave analysis for the scattering problem. On the other hand the signal duration should be sufficiently short such that the components reflected from the liquid-solid interface, and longitudinal and transverse waves scattered by the inclusion are separated in time.

It was also assumed that the inclusion is located at a depth greater than the Rayleigh wave influence zone and the reflected wave at the liquid-solid interface is not affected by the inclusion. Besides, in that theoretical analysis it was considered that the waves were scattered by the inclusion only once and the multiple scattering was ignored. The first wave from the cavity that is received by the transducer is the signal that is transmitted as the longitudinal wave into the solid and scattered by the cavity as the longitudinal wave as well. In the experiment it was found that the amplitude of this wave is much greater than that of all other waves and hence we restrict our consideration to this wave only.

Let the spherical inclusion center be placed at a vertical distance Z from the center of curvature of the transducer of half aperture angle α along the transducer axis and at a horizontal distance R from the transducer axis. The radius of the inclusion is a. The distance between the solid-liquid interface and the center of inclusion is D. Then the total output voltage V generated by the reflected signal from the liquid-solid interface and scattered waves from the inclusion, is equal to [14]:

$$V = \frac{2 V_0}{1 - \cos\alpha} \frac{\rho_s c_l}{\rho c} \sum_{n=0}^{\infty} \sum_{m=0}^{n} (-1)^n (2 - \delta_{0m}) \tau_m^{ll} L^2_{nm} \quad . \qquad (1)$$

Here V_0 is the output signal of the transducer when a perfect reflector is placed at the focal plane, ρ and ρ_s are the densities of the liquid and the solid respectively, c_l and c are the longitudinal wave speeds in the solid and in the immersion liquid, δ_{nm} is the Kronecker delta, and τ_n^{ij} are the scattering coefficients for the spherical inclusion [7,8].

The integral coefficient L_{nm} for the longitudinal wave depends on the inclusion position and elastic properties of the solid and can be expressed as

$$L_{nm} = (-i)^m \int_0^{\alpha} P(\theta) L(\theta) \exp(i\Phi_l) J_m(\eta) \overline{P}_n^m(\cos\theta_l) \sin\theta \, d\theta \quad . \qquad (2)$$

Here $P(\theta)$ is the pupil function of the lens, $L(\theta)$ is the transmission coefficient of a plane longitudinal wave traveling from the liquid to the solid [3], J_m is the m-th order cylindrical Bessel function of the first kind, $\overline{P}_n^m(\cos\theta_l)$ is the normalized associated Legendre polynomials. The position of the inclusion is determined by values of η, and Φ_l (η=kRsin θ, and Φ_l= $-kz_p\cos\theta + k_l D\cos_l\theta$), where k_l and k are wave numbers of the longitudinal waves in solid and in the immersion liquid, and $z_p = Z + D$ is the distance between the focus and the solid-liquid interface. The angles of propagation of the longitudinal wave in the liquid and the longitudinal and transverse waves in the solid are related by Snell's law $k \sin\theta = k_l \sin\theta_l$. Equations (1) and (2) are used to calculate both phase and amplitude of the received signal of a reflection acoustic microscope for spherical voids and inclusions in an elastic solid.

EXPERIMENTAL MEASUREMENTS

To determine the phase of the reflection coefficient one can obtain the phase of the received signal and compare it with the phase of another signal which is reflected from a reflector which has a known constant (independent of incident angle) value of the reflection coefficient. A good example of it is a free surface of a liquid. For proper comparison both reference surface and the surface under inspection must be at the same distance from the ultrasonic transducer. If this distance is of arbitrary value, as for defects in a material, it is still possible to determine the phase of the reflection coefficient if it is not frequency dependent. In this case the phase of the received signal is linearly dependent on the frequency because of a constant time shift between the starting point of the received signal and the gate position. It can be expressed as:

$$\phi = Af + \phi_0 \tag{3}$$

where ϕ_0 is the frequency independent phase shift which includes the phase shift due to reflection by the obstacle (defect). The slope (A) of the frequency dependent phase curve (ϕ) is proportional to the ultrasonic velocity in the medium [15]. The frequency dependence of the phase of the received signal can be affected by the arbitrary position of the receiving gate for swept frequency method or arbitrary window position for the broad band pulse system with the Fourier analysis [5].

For digital analysis of the received signal we used IBM PC compatible computer with Markenrich waveform acquisition and arbitrary generator board working with 20 MHz sampling frequency. The short pulse or sinewave video pulse was generated by Wavetek 395 arbitrary waveform generator, amplified by Matec 310 gated amplifier and supplied to 25 MHz PVDF focusing transducer (Panametrics ZF3002-SU). The transducer diameter was 10 mm and its radius of curvature was 9.5 mm. Stepper motor driving scanner was used as a positioning device with 6.35 μm accuracy and the first stage of Matec 605 broad band receiver was used as a preamplifier.

Tungsten carbide balls of 0.5 mm diameter, stainless steel balls of 1 mm diameter, and approximately 0.4 mm diameter air bubbles were used to model solid inclusions and void type defects. They were placed on a surface of weak gelatin jelly or incorporated in a polyester epoxy resin. The longitudinal ultrasonic wave speed of polyester epoxy as measured by the pulse echo method was 2600 m/sec. For the phase measurements both broad band pulse technique and frequency sweeping technique were used, they essentially gave the same

results. For the broad band pulse technique the received pulse was digitized and the phase component of the Fast Fourier Transform (FFT) of the time history was calculated.

For the frequency sweeping technique the received signal V(t) was digitized within a gate and phase shift between it and the carrier signal sin(2πft) was digitally calculated as:

$$\tan(\phi_0) = \sum [V(t)\cos(2\pi ft)] / \sum [V(t)\sin(2\pi ft)]. \quad (4)$$

The gate of a duration of one period of the lowest frequency was positioned about one cycle after the beginning of the signal to diminish the influence of the possible resonance scattering.

Phase-frequency curves for the 0.5 mm tungsten carbide ball and 0.4 mm air bubble in water are presented in fig.1. Their acoustic microscope generated images at 9 MHz frequency are shown in fig. 2. These images are generated by scanning the object in a vertical plane. Conventional C-scan images are generated by moving the microscope lens in a horizontal plane, say xy-plane, but these images are generated by moving the lens in a vertical plane say xz-plane which coincides with the vertical central plane of the spherical defect. One advantage of this image over conventional C-scan image is that from this image one can derive the diameter of the circular C-scan image of the defect for different vertical positions of the microscope lens. Hence it contains equivalent information of a large number of C-

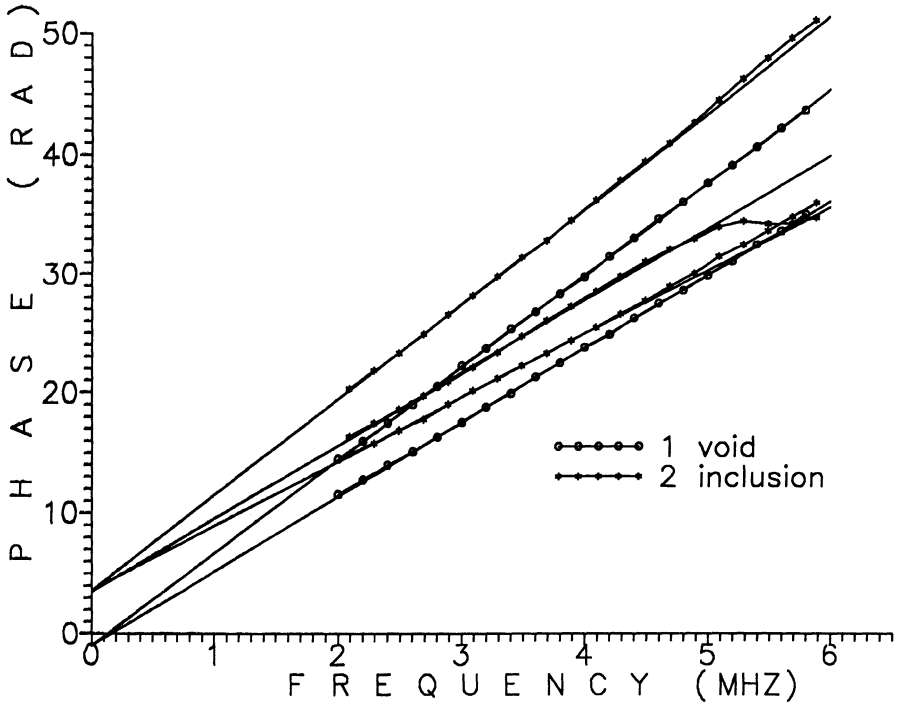

Figure 1: Phase-frequency curves for 0.4 mm air bubbles - (1) and 0.5 mm tungsten carbide balls - (2) in water. Two extreme curves for each case correspond to the axial shift of the ball by a distance of 1 mm.

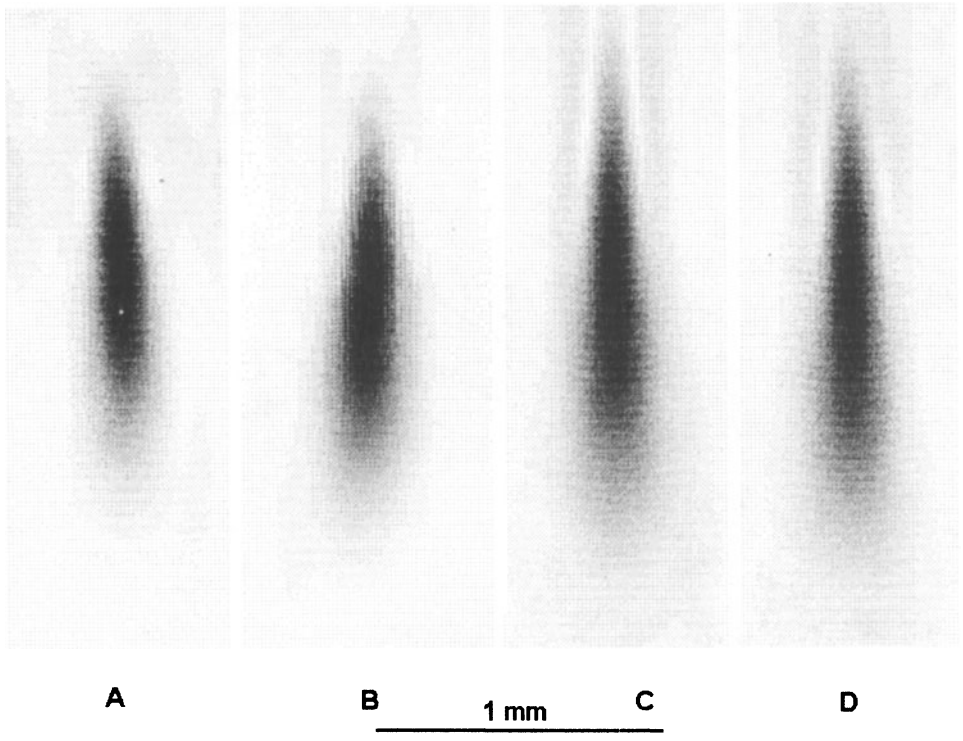

Figure 2. The acoustic microscope generated images of the tungsten ball in water - A, and at a 2 mm depth in polyester epoxy - B, and the air bubble in water - C, and at a 2 mm depth in polyester epoxy - D. Signal frequency is 9 MHz.

scan images. Images A and C are for the tungsten ball in water and at a 2 mm depth in polyester epoxy respectively. Images B and D are for the air bubble in water and at a 2 mm depth in polyester epoxy respectively. One can see that these images of air babble and solid inclusion are practically indistinguishable and more, it is not easy to determine the exact position of the inclusion with respect to the transducer focal point. But the constant part ϕ_0 in eqn. (3) of the phase of the received signal is not affected by its focal position as shown in fig. 1. In this figure different curves correspond to different transducer positions. For two extreme curves in each category the focal point of the transducer moved vertically along the central axis of the ball by a distance of 1 mm. The phase difference between the void and the solid inclusion reflected signals at zero frequency is slightly less than 180°, but still can be clearly noticed.

The experimental results for the air bubble or void and the tungsten carbide particle in an elastic solid is presented in fig. 3. They are located at 2 mm depth in polyester epoxy. Curve 1 is for 0.4 mm void, curve 2 is for 0.5 mm tungsten carbide particle and curve 3 is for 0.8 mm void. Several curves correspond to different focal positions of the transducer along the vertical central axis of the ball. The phase difference of 180° between the void and the inclusion can be clearly seen.

Corresponding theoretical curves generated by equations (1) and (2) for empty void and solid inclusion [7,8] are presented in fig. 4. The curves in fig.5 are obtained by subtracting the linear best fit curve from the curves in fig. 4.

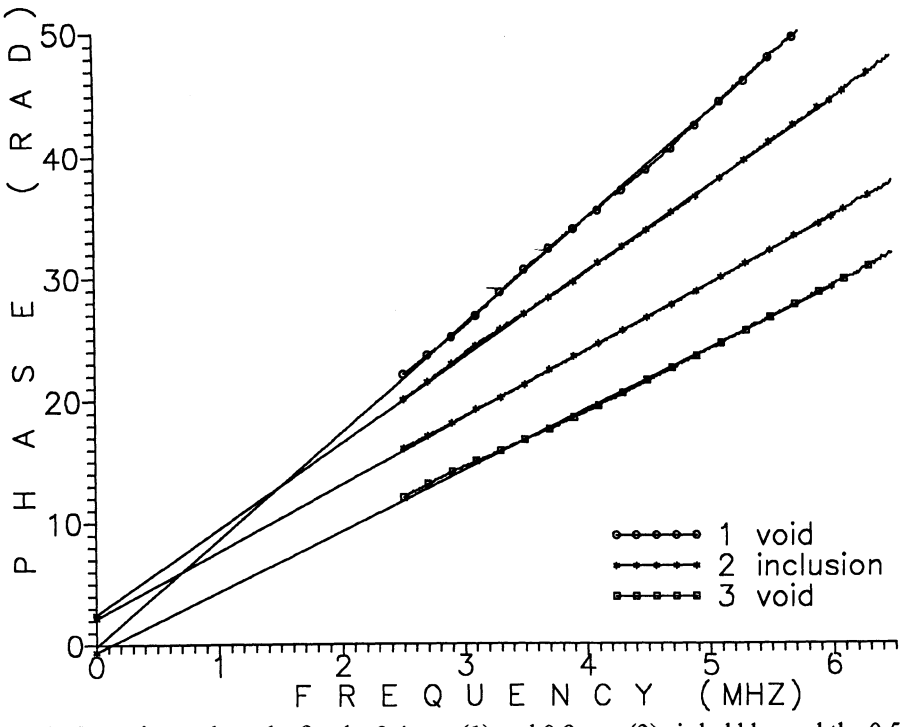

Figure 3. Experimental results for the 0.4 mm (1) and 0.8 mm (3) air bubbles and the 0.5 mm tungsten carbide ball (2) in polyester epoxy.

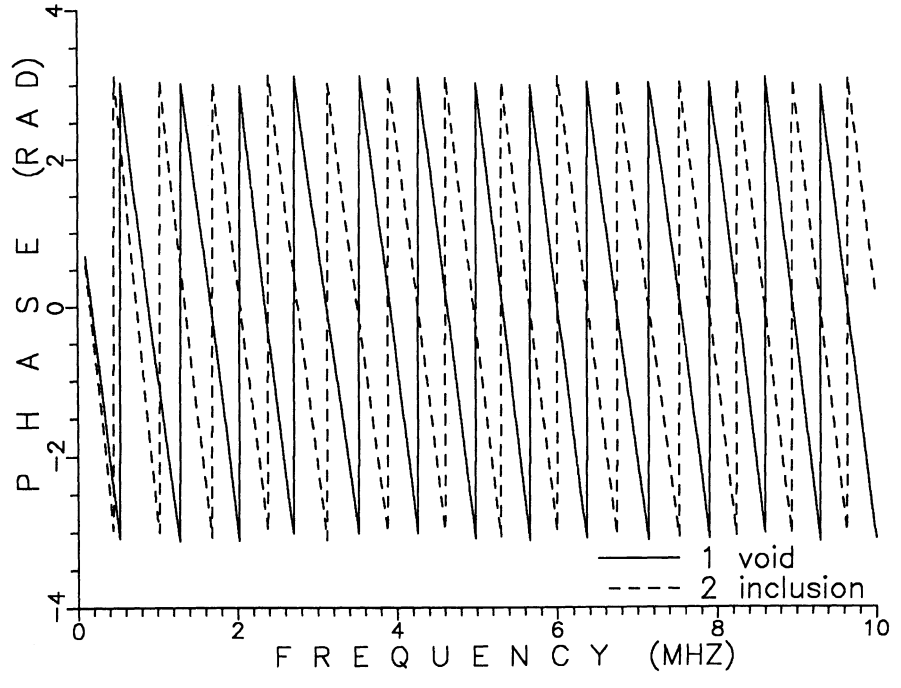

Figure 4. Theoretical curves, from equations (1) & (2), for void (1) and solid (2) inclusions

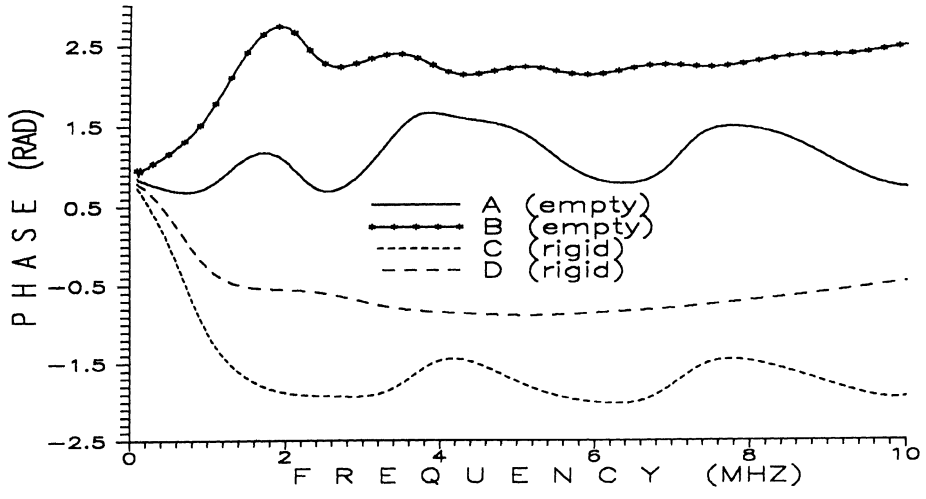

Figure 5: Theoretical curves for square pupil function for void (1) and solid inclusion (3) and for Sasaki pupil function - for void (2) and inclusion (4). The linear best fit curves are subtracted from the curves generated by equations (1)-(2).

The oscillations in the theoretical curve (curves A and C) are practically absent in the experimental curve in fig. 3. Similar result were obtained theoretically in previous works for the image of spherical particles [16] and V(z) curves for voids and inclusions in elastic solids [17]. Absence of the oscillations in the experimental phase-frequency curves is due to the fact that for an acoustic microscope lens the amplitude of the paraxial ray is much greater than the edge rays. Even for the spherical transducer the pupil function must gradually decay to zero near the transducer edge. Hence, one should use a proper pupil function to describe the focused beam. We use Sasaki pupil function $P(\theta)$ [18] in our calculations. This pupil function is defined as

$$P(\theta) = \begin{cases} (1+\cos(\pi(1-\cos\theta)/(1-\cos\alpha)))/2, & \text{if } \theta < \alpha \\ 0, & \text{if } \theta > \alpha \end{cases} \qquad (5)$$

The theoretical phase-frequency curves for tungsten carbide ball and void calculated with Sasaki pupil function are shown by curves B and D in figure 5. One can see that the phase difference is approximately 180° between the void and the solid inclusion at a frequency grater than 2 MHz (ka>1) similar to the experimental results (figure 3), thus good agreement between experimental and theoretical results is achieved.

CONCLUSION

The phase of an acoustic microscope input signal when its lens is focused on the spherical obstacle in an elastic material can be used to obtain the phase of the reflection coefficients of the obstacle. If ka>1 it is possible to distinguish inclusions with acoustic impedance higher than that of the surrounding material from void with acoustic impedance lower then that of the surrounding material. The influence of the possible resonance scattering can be diminished by choosing the appropriate acquisition gate position near the beginning of a received echo signal. Simple models were used in the experiment to show that the phase difference between reflected signals from voids and inclusions is 180° at zero frequency.

ACKNOWLEDGMENT

This research was supported by the NATO linkage grant program HTECH.LG 931353 and NSF equipment grant MSS - 9310528. Authors would like to thank professor V.K. Kinra for providing the tungsten carbide and steel balls and for helpful discussions.

REFERENCES

1. A. Briggs, "Acoustic Microscopy", Clarendon Press, Oxford, 1992.
2. J. Krautkramer, H. Krautkramer "Ultrasonic testing of materials" Springer-Verlag, Berlin Heidelberg, N.Y. 1983., p. 536.
3. L.M. Brekhovskikh, "Waves in layered media" Academic Press, N.Y., 1960.
4. W.A. Simpson Jr., "Time-Frequency-Domain Formulation of Ultrasonic Frequency Analysis", J. Acoust. Soc. Am. 5 (6) pp. 1776-1781 , (1974).
5. D.E. Fitting, L. Adler, "Ultrasonic Spectral Analysis for Nondestructive Evaluation", Plenum, N.Y. 1981, pp.106-109.
6. N. Nakaso, K. Ohira, M. Yanaka, Y. Tsukahira, "Measurement of acoustic reflection coefficient by an ultrasonic microspectrometer", IEEE trans, ultrason. ferroelectr. Freq. Control, 41 (4) pp. 494-502, (1994).
7. C.F. Ying and R. Truell, "Scattering of a plane longitudinal wave by a spherical obstacle in an isotropically elastic solid", J. Appl. Phys. 27, pp. 1086-1097, (1956).
8. N.G. Einspruch, E.J. Witterholt and R. Truell, "Scattering of a plane transverse wave by a sphrrical obstacle in an elastic medium", J. Appl. Phys., 31, pp.806-818 (1960).
9. J.E. Gubernatis, E. Domany, J.A. Krumhansl, M. Huberman, "The Born Approximation in the Thery of the Scattering of Elastic Waves by Flaws", J.of Appl. Phys., 48 (7), pp.2812-2819 (1977).
10. B.R. Tittmann, R.E. Cohen. J.M. Rochardson, "Scattering of Longitudinal Waves I ncident on Spherical Cavity in a Solid", J. Acoust. Soc. Am. 63 (1) pp. 68-74, (1978).
11. A. Stockmann, P.S. Nocholson, "Ultrasonic Characterization of Model Defects in Ceramics - Voids in Glass - Theory and Practice", Mat. Eval., 44 , pp.756-761, (1986).
12. A. Stockmann, P. Mathieu, P.S. Nocholson, "Ultrasonic Characterization of Model Defects in Ceramics (part 3). Spherical Inclusion in Opaque Crystallized Glass - Theory and Practice, Materials Evaluation", 47 (3) pp. 356-362, (1989).
13. O.I. Lobkis and P.V. Zinin, "Acoustic microscopy of spherical objects. Theoretical approach", Acoust. Lett. 14, 168-172,(1991).
14. O.I. Lobkis, T. Kundu, and P.V. Zinin "A theoretical analysis of acoustic microscopy of spherical cavities". Wave Motion 21, pp. 183-201, (1995).
15. L. Paradis, J.F. Salin, "Non destructive evaluation of the mechanical characteristics of plasma sprayed ceramic coatings" in Review of progress in quantitative nondestructive evaluation, 13B eds. D.O. Thompson and D.E. Chimenti, Plenum N.Y. 1994, pp. 1229-1236.
16. O.V. Kolosov, O.I. Lobkis, K.I. Maslov, P.V. Zinin, "The effect of the focal plane position on the images of spherical objects in the reflection acoustic microscope", Acoust. Lett. 16, pp. 84-88 (1992).
17. O.I. Lobkis, K.I. Maslov, T. Kundu, P.V. Zinin, "Spherical Inclusion Characterization by the Acoustic Microscope: Axisymmetric Case", J. Acoust. Soc. Am, in press (1995).
18. Y. Sasaki, T. Endo, T. Yamagishi and M. Sakai, "Thickness measurement of a thin film layer on an anisotropic substrate by phase-sensitive acoustic microscope", IEEE Trans. UFFC. 39, pp. 638-642 (1992).